A Survey on the Implementation of a Magnetic Induction Tomography Prototype: Theoretical Description and Experimental Issues

Nuno B. Brás[1], Raúl C. Martins[2], António C. Serra[3]
[1-3]Instituto de Telecomunicações
Instituto Superior Técnico, Torre Norte, Piso 10
Tel: +351 218418489, Fax: +351 218417672,
e-mail: [1]nuno.bras@lx.it.pt, [2]rcmartins@lx.it.pt, [3]acserra@ist.utl.pt

Abstract — **Magnetic Induction Tomography (MIT) is an imaging technique that allows mapping the complex conductivity structure of a body. Besides industry, its application to biological tissues has been recently studied. Work was done by the authors in order to project, build and assess a new MIT system for biological purposes. Three distinct areas are investigated: The parameter estimation problem solver, the forward problem solver and the experimental design and dimensioning. In this paper, a description of the main motivations that steered the development of each of these working areas is presented. A theoretical explanation of the overall process and considerations about further work are also depicted.**

I. INTRODUCTION

Magnetic Induction Tomography (MIT) [1] is an imaging technique for passive electrical properties based in measuring induced magnetic fields inside the body in analysis imposed by an external magnetic field source, allowing reconstruction of its internal structure. In the case of biological tissue bodies, the major electrical property to be characterized is the complex conductivity. Bodies to be analyzed have some tens of centimeters, characterized by small changes on conductivity between adjacent tissues, typically 0.5 to 2 S/m. Frequencies ranging from some tens of kHz to some MHz are used in the excitation magnetic field, inducing eddy currents inside the object that will generate a magnetic field, which should be measured. A parameter estimation problem based on these measurements is then solved in order to reconstruct the body conductivity map.

This imaging method received special attention in recent studies due to the fact that, contrarily to what happens with the classical Electrical Tomography, magnetic field is not shielded by bone regions, allowing it to access the entire body map. Moreover, its low cost and sensor connectionless are also relevant properties.

Classical experimental setups allow acquiring a fixed number of sensing coils placed in specific positions [2] (see Fig 1, left side, to understand the geometrical shape of a typical MIT setup). Moreover, typically the same number of coils sources in the same geometric position is used. For example, for a set of 8 coils of each type, a total of 56 measurements are obtained, since the same position can't be sensing and source simultaneously, which is a small number for the involved volume and conductivity map complexity.

The central idea of this research has been to improve the reconstructed parameter map by making more independent measurements using additional incident angles of the source magnetic field over the body in test and improving the angular acquisitions between the object and the sensing coils. Also, the performance of the parameter estimation solver has been also an issue, since it is known to be a very time consuming process, and this will become even more critical if a larger set of measured data is used.

Following this perspective, the research areas that have been focused are: (i) the eddy current problem 3D simulator, working as a simulator of the experiment scenario or as a component of the parameter estimation solver; (ii) the parameter estimation model, which solves the imaging problem itself; (iii) the experimental setup. This paper summarizes the advances made in these areas, showing the research complexity of each one.

II. RESEARCH AREAS

A. The Parameter Estimation Model

Soft fields parameter estimation problems are a specific case of large variable set inverse problems. The MIT problem is an ill-posed non linear optimization problem that could be stated as [3]:

$$F(\sigma^*) = d \tag{1}$$

Where d the measured array of data and $F(\sigma^*)$ is the so called parameter-to-observation map or forward function.
The ill-posedness of the operator F and the data corruption by noise forces to redefine the solution as the minimum of the following minimization problem:

$$\sigma^* = argmin_\sigma \ \|F(\sigma) - d\|^2 + \alpha J(\sigma) \tag{2}$$

J is a regularization term that introduces *a-priori* knowledge about the σ map shape. A Total Variation regularization method was used in this study (see [3] and references therein). In the MIT case, this equation should be written as:

$$\sigma^* = argmin_\sigma \ \textstyle\sum_i \|\mathbf{M}\mathrm{u_i}(\sigma) - d_i\|^2 + \alpha J(\sigma) \tag{3}$$
$$s.t. \ \mathbf{A}(\sigma) u_i = y_i$$

Where $\mathbf{A}$ is the forward operator (the PDE equation) that maps fields (u_i) into their sources (y_i) and $\mathbf{M}$ is the measure

This work was sponsored by the FCT research project POSC/EEA-ESE/60397/2004.

matrix that in the MIT case integrates the field over the sensing coils, generating the electromotive force that is experimentally measured. These measurements are represented by d. The setup of a real MIT system implies to impose several positions of the magnetic source that is why this problem is the summation of each i acquisition context.

There are a few different approaches to solve the problem defined by (3). A commonly used method is to substitute the equality constraining in the main expression, resulting in:

$$\sigma^* = \ argmin_\sigma \ \sum_i ||\mathbf{MA}^{-1}(\sigma)y_i - d||^2 + \alpha J(\sigma) \quad (4)$$

In a large scale problem case, a known option is to apply a Truncated Newton Method (TNM) [4]. It is a family of large scale problem methods where the solution is found solving two iterative problems: (i) a main iteration stated by the Gauss-Newton method; (ii) For each of these iterations, an iterative evaluation of the step direction, k=$\boldsymbol{H}^{-1}G$, is done solving the linear problem $\boldsymbol{H}k = G$ using the Preconditioned Conjugate Gradient (PCG) method, where $\boldsymbol{H}$ is the resulting Hessian and G is the gradient. This was the adopted method to solve the inverse problem.

B. The Forward Problem

Each iterating step of the parameter estimation problem, forces to solve several forward problems that is, a set of 3D eddy current Partial Differential Equations (PDE) that models the fields from sources and parameters. They are typically solved using approximated discrete techniques. In this research, it has been followed the idea that the forward solver should be fast even if that requires losing the shape correctness. The orthogonal meshing with multiple resolution volumes has a very quick global stiffness matrix construction making this approach an interesting candidate to fulfill the place of a forward problem solver. Commercial solvers are not optimized to work as inverse problem iterations. Used matrices in the forward problem are fundamental in the solution of the inverse problem. The access to matrices morphology, derivatives and second (Gauss-Newton) derivatives of the forward problem matrix are fundamental to solve the inverse problem. This led to a complete development of a 3D eddy current platform.

Given the MIT context, the used approach to solve each PDE problem was to consider a linear, quasi-static approximation, and to solve a harmonic description of Maxwell equations. Other two characteristics and simplifications were considered: (i) isotropy of the complex conductivity strongly reduces the ill condition of the problem, turning the reconstruction much more feasible. All models in literature are based in this simplification, e.g. [1]. (ii) constant magnetic permeability (μ) is generally accepted when studying magnetic properties of biological tissues excepting on specific pathologies. The electric description of the general eddy current law for constant permeability problem is now stated by substituting the Faraday Law of induction in the Ampere's law, defined in the harmonic formulation:

$$\nabla \times \nabla \times \boldsymbol{E} + \ i\omega\mu\boldsymbol{\sigma}\boldsymbol{E} = \ -i\omega\mu\boldsymbol{J_s} \quad (5)$$

The electric scalar potential (ϕ) and Magnetic vector potential ($\boldsymbol{A}$) are used to solve this problem because they are continuous function with continuous second derivative (C^2). The potentials are defined by the Helmholtz decomposition $\boldsymbol{E} = -i\omega(\nabla\phi + \boldsymbol{A})$ and the relation $\boldsymbol{B} = \nabla \times \boldsymbol{A}$. After some algebra, the following relation is obtained:

$$\nabla \times \nabla \times \boldsymbol{A} + \ i\omega\mu\boldsymbol{\sigma}(\nabla\phi + \boldsymbol{A}) = \ \mu\boldsymbol{J_s} \quad (6)$$

The Coulomb gauge ($\nabla \cdot \boldsymbol{A} = 0$) allows to uniquely define $\boldsymbol{A}$. Using it in $\nabla \times \nabla \times \boldsymbol{A} = \nabla(\nabla \cdot \boldsymbol{A}) - \Delta\boldsymbol{A}$ and substituting the resulting expression in (6) gives:

$$\Delta\boldsymbol{A} - i\omega\mu\boldsymbol{\sigma}\boldsymbol{A} = -\mu\boldsymbol{J}_s + \ i\omega\boldsymbol{\sigma}\nabla\phi \quad (7)$$

The current continuity equation should then be added to the system of equations, establishing the following relation:

$$\nabla \cdot [i\omega\boldsymbol{\sigma}(\nabla\phi + \boldsymbol{A})] = 0 \quad (8)$$

The $\boldsymbol{A_r}$, $\boldsymbol{A_r}$-ϕ description where $\boldsymbol{A} = \boldsymbol{A_r} + \boldsymbol{A_s}$, allows to impose current sources by defining imposed potential $\boldsymbol{A_s}$ along the space. Here, $\boldsymbol{A_s}$ is calculated using the Biot-Savart Law applied in a cylindrical coil. The equations (11) and (12) take the form:

$$\Delta\boldsymbol{A_r} - i\omega\mu\boldsymbol{\sigma}\boldsymbol{A_r} - i\omega\boldsymbol{\sigma}\nabla\phi = i\omega\mu\boldsymbol{\sigma}\boldsymbol{A_s} \quad (9)$$

$$\nabla \cdot [i\omega\boldsymbol{\sigma}(\nabla\phi + \boldsymbol{A_r})] = -\nabla \cdot i\omega\boldsymbol{\sigma}\boldsymbol{A_s} \quad (10)$$

Homogenous Dirichlet boundary definitions are considered, forcing $\nabla \cdot \boldsymbol{A_r} = 0$. The equations were discretized using a Finite Volume based method, similar to a Yee scheme on a staggered cell complex, resulting in:

$$\mathrm{lap}\ \hat{a}_r - i\omega\mu\sigma\ \hat{a}_r - i\omega\sigma\ \mathrm{grad}\ \phi = \ i\omega\mu\sigma\ \hat{a}_s \quad (11)$$

$$\mathbf{div}\,[i\omega\boldsymbol{\sigma}(\ \mathbf{grad}\ \phi + \hat{\boldsymbol{a}}_r)] = -\mathbf{div}(i\omega\boldsymbol{\sigma}\hat{\boldsymbol{a}}_s) \quad (12)$$

Where $\hat{\boldsymbol{a}}$ and $\boldsymbol{\sigma}$ are defined over the cell facets and ϕ is defined over the cell centre. For further reading about this topic, see e.g., [5]. The OcTree cell subdivision or subgridding was developed, allowing having higher resolution zones without imposing non-orthogonal cells. The problem $\mathbf{A}(\sigma)u_i = y_i$ is now defined by (15) and (16), where each u_i is a coordinate based sorted array of Magnetic and Electrical Potentials. A Forward solution of this problem typically solved by iterated approximated methods instead of direct ones. The results were obtained using the BiConjugate Gradients Stabilized (BiCGStab).

C. The Experimental Prototype

If the idea of in-vivo imaging is relaxed, sensors could be moved around the object allowing acquiring data from more positions and new incident angles of the source field. Following this idea, a prototype that allows rotating the sensing coils and rotating and moving vertically the body plate was designed in order to study image reconstruction using an optimum set of measurements for each body in analysis. A new cancelation technique called here as Twin Coils Setup was developed before and implemented in this prototype. The novelty consists in placing the source at the centre of a circular setup, and the sensing coils positioned at opposite sides of the circular layout. The half circle where the object is placed is then measured differentially, in relation to the opposite half circle. In Fig. 1, the classical architecture and the new one are presented side by side.

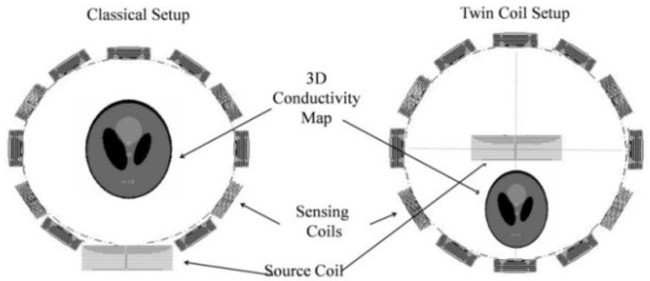

Fig.1. Comparison between a classical geometry and the Prototype Geometry, upper view.

Depending on the source field generator, acquisitions should have a noise standard deviation between tens to hundreds of nanoVolts. Details on the measurement necessities and advantages of this design are available in [6]. Each acquisition should be preceded by a calibration step that measures the residual signal for each position. Two main challenges arising from such a MIT moving system: (i) sensing coils mechanical positioning should be precise enough so that measures are not affected by positioning errors, since the calibration should be done exactly in each acquiring position; (ii) in order to have a set of useful measures, the system should be stable during all the acquisition period of time. A Photo of the developed prototype is presented in Fig.2:

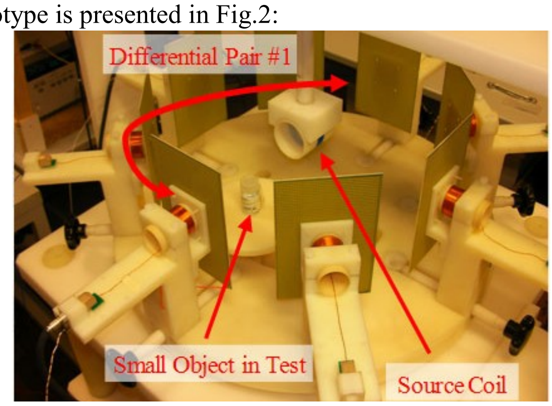

Fig.2. Photo of the Developed Prototype

III. RESULTS

A. Testing the 3D Forward Problem Solver

The solver was validated by two distinct ways. Firstly, the observation of the current lines should close inside the object. A thin card was simulated in a parallel angle to the source coil, allowing analyzing the induced currents. In the next figure such a simulation is shown, where it is possible to see the current line vector field in green defined just inside the plate. The color map describes the current intensity.

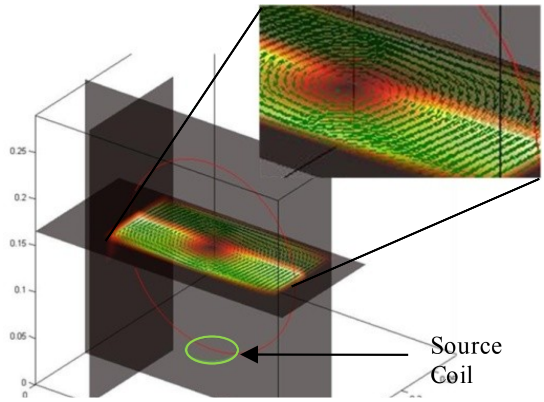

Fig.3. Current density observation, in the case where a finite plane is orthogonal to the source coil axis

Secondly, an analytical model is used to compare results. A known geometry that has a close solution of the eddy current problem is given by the geometric setup also used in the previous Fig. 3 but with an infinite conductive layer, radiated by a magnetic field from a source coil. In [7] a detailed explanation is given about this analytical solution. In Fig. 4, a relative error is shown that relates the analytical electromotive voltage picked by this sensing coil in an infinite layer condition and the corresponding numerical simulation where large finite plates are used. This relative error figure is shown for several distances between a sensing coil and the infinite conductive layer (each x coordinate) and for several large finite plates (each plot).

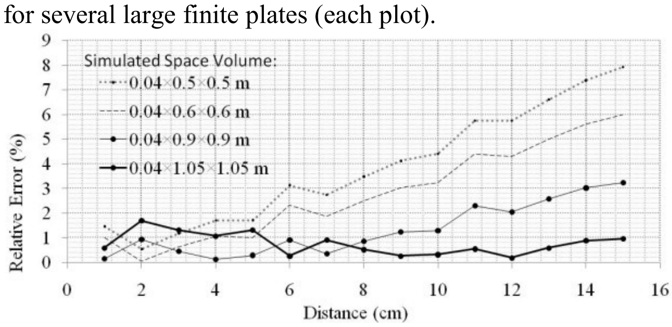

Fig.4. Relative error of four layer dimension simulations, for a sensing coil measurement done

The visible trend for higher distances is due to approximating an infinite layer by a finite plate. For the larger plate, this trend is not seen, which means that the ~1.5% resultant error is mostly the method intrinsic error.

B. Implementation Results of a 2D Parameter Estimation Solver

The first implementation was focused in developing a framework to test several methods in a reasonable amount of time. In this sense, an eddy current problem solver for the 2D case was developed using a reduced version of the developed 3D forward problem, keeping however its matricial properties. This allowed to implement a simple and yet fully featured eddy current parameter estimation solver. In morphological terms, the involved matrices are quite similar but faster to manipulate. In terms of the stated physical problem, it is a *xy* slice of a space constant in *z*, where all the generated magnetic vector potentials are aligned over that plane, as well as the source and sensing coils. The space in analysis is presented in Fig. 5. A preliminary result is shown where a set of 10 source coils and 200 sensing points chosen inside the red circumference were used, with 0.1% measurement noise.

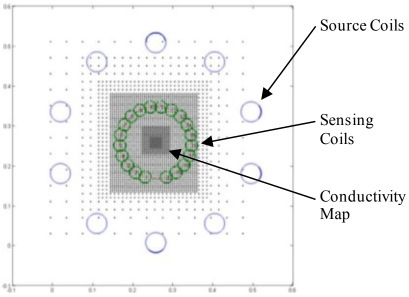

Fig.5. A 2D Space in analysis of a simple square with 3 different conductivity coefficient levels.

The source coils are turned on consecutively and for each one, the sensing measurements are taken. A first result on this reconstruction using the referred TNM method is presented in the Fig.6. Note that the original and the reconstructed ε is constant and equal to zero.

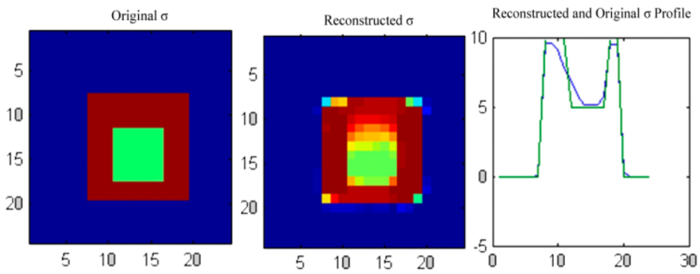

Fig.6. Reconstructed 2D image of a simple square with 3 different conductivity coefficient levels.

C. The Experimental Setup Stability Signal

A challenge of the experimental setup is to keep the system stable during all the acquisition period of time. Here we present a unique acquisition from a differential sensing coil, during 300 seconds, without any object placed in the system.

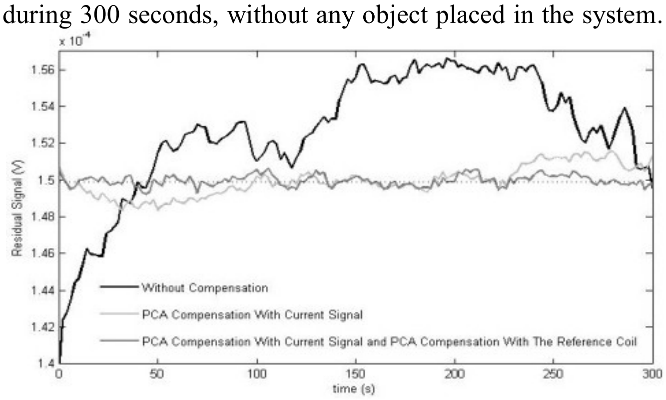

Fig.7. Signal acquisition, using a source current signal to cancel drifts and using also a reference coil.

The raw acquired signal is the black line. The dark gray signal is compensated with the current deviation, measured from the source coil, which clearly influences the measurement value along time. Standard deviation of the corrected signal was of 500 nV. The light gray signal is compensated not just with the current deviation signal but also with a reference coil signal. Resulting signal was even more stable, with a standard deviation of ~100 nV. Principal component analysis was used to implement both compensations. Influence of the compensations in the final measures has yet to be evaluated.

IV. Conclusions And Further Work

Each research area of the MIT prototype design was summarized in terms of results. The simulator is working with 1.5% maximum relative error. A 2D framework inverse problem solver is now working and preliminary results were shown. The new prototype measuring system is also working in a acceptable level of noise (hundreds of nanoVolts), although further tests should be done to support the used methods.

The next steps in the development of the system include finishing the sensing coil angular positioning control unit, a new source field amplifier and a new acquisition signal amplification stage for all sensing coils. This will allow having measurements from several angular positions, as planned. Furthermore, analysis of the geometric space, using the developed 3D model will start to be done in order to look for numerical improvements to the new geometrical setup. Finally, the implementation of a stable 3D parameter estimation solver using TNM is being finished. Implementation of other numerical methods is now scheduled.

References

[1] H. Griffiths, W.R. Stewart, "Magnetic Induction Tomography, a measuring system for biological tissues", Ann. NY Acad. Sci. no. 873, pp. 335-345, 1999.

[2] H Scharfetter, "Hardware for quasi-single-shot multifrequency magnetic induction tomography (MIT): the Graz Mk2 system", Phys. Meas. 29 S431-S443, 2008

[3] Curtis R. Vogel, "Sparse matrix computations arising in the distributed parameter identification", SIAM J. Matrix Anal. Appl., 20, 1027-1037,1999.

[4] Stephen G. Nash, "A survey of truncated- Newton Methods", Journal of Computational and Applied Mathematics, 124, 45-49, 2000.

[5] Eldad Haber, Stefan Heldmann, "An octree multigrid method for quasi-static maxwell's equations with highly discontinuous coeficients", Journal of Computational Phyisics, 223, 783-796, 2007

[6] Nuno B. Brás, Raul C. Martins, Antonio C. Serra, "Characterization of a new symmetrical cancelation method for magnetic induction tomography", 16th IMEKO TC4 Intern. Symp. Proceedings, 922-927, 2008.

[7] C.V. Dodd, W.E. Deeds, "Analytical Solutions to Eddy-Current Probe-Coil Problems", Journal of Applied Physics, 39 , 2829-2838,1968.